

GlyphMastero: A Glyph Encoder for High-Fidelity Scene Text Editing

Tong Wang^{1,†}, Ting Liu^{1,†}, Xiaochao Qu¹, Chengjing Wu¹, Luoqi Liu^{1,✉}, Xiaolin Hu^{2,✉}

¹ MT Lab, Meitu Inc., Beijing 100083, China

² Department of Computer Science and Technology,
BNRist, IDG/McGovern Institute for Brain Research,
Tsinghua University, Beijing 100084, China

{wt6, lt, qxc, ethan, llq5}@meitu.com

xlhu@tsinghua.edu.cn

[†]Joint first authors. [✉]Joint corresponding authors.

Abstract

Scene text editing, a subfield of image editing, requires modifying texts in images while preserving style consistency and visual coherence with the surrounding environment. While diffusion-based methods have shown promise in text generation, they still struggle to produce high-quality results. These methods often generate distorted or unrecognizable characters, particularly when dealing with complex characters like Chinese. In such systems, characters are composed of intricate stroke patterns and spatial relationships that must be precisely maintained. We present GlyphMastero, a specialized glyph encoder designed to guide the latent diffusion model for generating texts with stroke-level precision. Our key insight is that existing methods, despite using pretrained OCR models for feature extraction, fail to capture the hierarchical nature of text structures - from individual strokes to stroke-level interactions to overall character-level structure. To address this, our glyph encoder explicitly models and captures the cross-level interactions between local-level individual characters and global-level text lines through our novel glyph attention module. Meanwhile, our model implements a feature pyramid network to fuse the multi-scale OCR backbone features at the global-level. Through these cross-level and multi-scale fusions, we obtain more detailed glyph-aware guidance, enabling precise control over the scene text generation process. Our method achieves an 18.02% improvement in sentence accuracy over the state-of-the-art multi-lingual scene text editing baseline, while simultaneously reducing the text-region Fréchet inception distance by 53.28%.

1. Introduction

Text editing is a task that, given a selected text region, replaces existing text content with new user inputs. The most



Figure 1. Example results of our scene text editing method on random images collected from the internet. The original images (left column) show source text regions marked with red boxes, with target texts displayed at the bottom left. The edited results (right column) demonstrate our method’s ability to preserve both structural accuracy and style consistency through stroke-level guidance across different visual styles and writing systems.

straightforward approach involves a two-stage process: text removal followed by font-matched text insertion. While this approach may suffice for images with printed texts, it

requires substantial expertise in font recognition to maintain style consistency. Moreover, for text in natural scenes (i.e. scene texts), this approach faces great challenges: even with perfect font identification, achieving visual coherence between the inserted text and the scene remains infeasible due to complex environmental factors such as perspective distortions, lighting conditions, and surface properties.

This challenge motivates the task of scene text editing, a special task within image editing domain that aims to modify texts in images while preserving the original style and maintaining visual coherence with the surrounding environment. Advances in this field benefits both everyday users and professional designers, particularly when they deal with typefaces that are either difficult to identify or impossible to replicate through conventional means.

Toward this end, diffusion-based [4] scene text editing methodologies [1, 2, 6, 25] have demonstrated significant potential to meet these demanding requirements. DiffUTE [1], a specialized scene text editing framework built upon diffusion models, exemplifies this approach. In contrast to text-to-image generation approaches that utilize text encoders such as CLIP [14] for extracting text embeddings from descriptive languages to enable language-driven generation, the framework employs features extracted by a pre-trained OCR model from rendered text lines as the glyph guidance for scene text editing. While DiffUTE achieves robust style preservation through its conditional inpainting formulation and demonstrates effective text editing capabilities for scenes with simple printed text, it shows significant limitations in text legibility when handling complex glyph structures such as Chinese characters (Figure 5). These limitations stem from the insufficient representational capacity of its OCR feature utilization in encoding intricate glyph structures.

To address the challenge of creating robust glyph representations for achieving precise scene text editing results, we propose *GlyphMastero*, a novel trainable glyph encoder that generates fine-grained glyph guidance for scene text editing. Our glyph encoder distinguishes itself through its explicit modeling of hierarchical relationships between local character-level glyph features and global text-line structures. By capturing these hierarchical relationships and using them for glyph feature generation, our approach enables more nuanced glyph representation learning. Additionally, we incorporate multi-scale OCR features through a feature pyramid network (FPN) [10] to enhance the representation of global text structures.

We adopt the inpainting-based formulation similar to DiffUTE as our generation backbone and train it with the glyph guidance from our *GlyphMastero*, achieving substantial performance improvements across writing systems ranging from Latin scripts to complex logographic systems such as Chinese characters. Both quantitative and qualita-

tive evaluations validate the effectiveness of our approach. In Figure 1, we present editing results on various images collected from the internet.

2. Related Work

Existing approaches for scene text editing can be broadly categorized into two paradigms: *GAN-based methods* and *diffusion-based methods*, each employing different strategies for conditioning the generative models.

2.1. GAN-Based Methods

Early approaches in the domain of scene text editing were predominantly based on Generative Adversarial Networks (GANs) [3]. Among these early works, STEFANN [18] introduced a dual-model architecture that combined a font-adaptive model for maintaining structural integrity with a dedicated style transfer network. In a different approach, MOSTEL [13] advanced the field by incorporating explicit stroke guidance maps to precisely delineate editing regions, while implementing a semi-supervised learning strategy that leveraged both synthetic and real-world data to enhance the model’s generalization capabilities. In parallel, several other GAN-based methodologies [5, 8, 26, 27] explored various architectural modifications to improve the quality of text generation. Nevertheless, these GAN-based approaches consistently encountered significant challenges when dealing with complex text structures and diverse style variations, frequently resulting in generated text that exhibited unrealistic characteristics and compromised visual quality.

2.2. Diffusion-Based Methods

Diffusion models have recently shown superior capabilities in modeling complex data distributions, making them well-suited for scene text editing tasks. These methods primarily differ in their conditioning strategies, which can be categorized into two types: cross-attention guidance and latent space guidance.

Cross-attention mechanisms have proven effective for conditioning diffusion models with additional information in scene text editing. DiffSTE [6] employs a character encoder for glyph information alongside CLIP [14] encoded instructions. AnyText [24] integrates OCR-extracted neck features from glyph images with CLIP-encoded descriptions. DiffUTE [25] utilizes fixed-length features from TrOCR’s [9] final hidden state. Building on DiffUTE, we replace text embeddings with glyph guidance through our novel trainable glyph encoder for comprehensive glyph representations.

Latent space guidance, popularized by ControlNet [30], introduces conditioning signals into diffusion models by encoding input conditions through convolutional layers and incorporating them into latent representations. Several

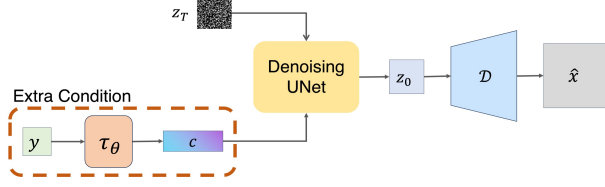


Figure 2. General pipeline for conditioning latent diffusion models with additional guidance signals. An extra condition y is processed through a condition encoder τ_θ to produce a condition embedding c . This embedding guides the denoising UNet via cross-attention during the iterative denoising process, which transforms the noisy latent z_T into a clean latent representation z_0 over T steps. Finally, an image decoder \mathcal{D} converts the latent representation z_0 into the final predicted conditioned image \hat{x} .

works in text generation [2, 11, 24, 28] have explored adapting this approach for scene text editing. TextDiffuser [2] implements character-level segmentation masks for fine-grained control, while GlyphControl [28] and AnyText [24] introduce indirect latent conditioning through feature concatenation. While these methods demonstrate success in text generation, their reported results suggest limitations in achieving style coherency in scene text editing. Specifically, the generated text style is typically constrained by the typeface used to render the glyph images provided as latent guidance. Based on these observations, we opt for a cross-attention-based approach paired with an inpainting formulation for scene text editing, which enables more precise control over glyph-level features while maintaining style coherence.

3. Method

3.1. Preliminaries

Diffusion models work by gradually adding noise to data and then learning to reverse this process. The DDPM model [4] was among the first to demonstrate the effectiveness of diffusion models for image generation, establishing foundational principles that subsequent models have built upon. Latent diffusion models [16] (LDMs) improved upon DDPM by operating in a compressed latent space rather than directly on pixels. They first encode images into a more compact representation, apply the diffusion process, then decode back to full images. This approach is more computationally efficient than denoising in the pixel space, making it practical for real-world applications. The training objective of LDMs is to minimize:

$$L_{\text{LDM}} := \mathbb{E}_{\mathcal{E}(x), c, \epsilon \sim \mathcal{N}(0,1), t} \left[\|\epsilon - \epsilon_\theta(z_t, c, t)\|_2^2 \right] \quad (1)$$

where \mathcal{E} is the encoder that compresses x to get latents z , ϵ represents the ground truth noise that is added to z in the forward pass, ϵ_θ is the time-dependent model that predicts

the noise added given time step t , realized by a UNet [17], and c represents the conditioning embeddings that guide the denoising process with the cross-attention mechanism. The extra conditioning embeddings c is usually acquired by encoding the extra condition y through a condition encoder τ_θ that transforms it into an embedding space, such that $c = \tau_\theta(y)$ (Figure 2). Once the denoising process is finished, the clean latent feature z_0 is decoded through a decoder \mathcal{D} to get the image $\hat{x} = \mathcal{D}(z_0)$.

The conditioning mechanism illustrated in Figure 2 can be exemplified through the case of text-guided image generation. In this context, the condition y comprises natural language descriptions (or text prompts) which are processed through a τ_θ that encodes texts. This encoder is typically implemented using language models, such as CLIP’s [9] text encoder or T5 [15]. The resulting text embedding $c = \tau_\theta(y)$ serves as a guidance signal for the UNet through the cross-attention mechanism. Upon completion of the denoising process, the model yields a refined latent representation z_0 that is conditioned on descriptive languages, and is subsequently transformed into the final image through the image decoder, often realized by a VAE [7] decoder, to get the generated image $\hat{x} = \mathcal{D}(z_0)$. This cross-attention guided architecture enables the text-to-image diffusion model to learn mappings between arbitrary textual descriptions and their corresponding visual representations during the iterative denoising procedure.

Many practical applications require modifying specific parts of an image rather than generating entirely new ones. While text-to-image diffusion models excel at global image generation, they need to be extended to support such granular control over specific image regions. For text-guided inpainting, Rombach *et al.* [16] followed LaMa [23] by introducing additional channels to process a binary mask m that indicates regions to be modified. Specifically, given a binary mask m , they first calculate:

$$x_m = x \odot (1 - m) \quad (2)$$

where x denotes the input image, and \odot denotes the Hadamard (element-wise) product. This operation effectively masks out (sets to zero) the regions marked for inpainting. The latent representation at timestep t , denoted as z_t , is then augmented by concatenating it with the mask m and the encoded masked image $\mathcal{E}(x_m)$, resulting in:

$$\hat{z}_t = [z_t; m; \mathcal{E}(x_m)] \quad (3)$$

where $\mathcal{E}(\cdot)$ is the image encoder function and $[\cdot]$ denotes channel-wise concatenation. The inpainting formulation generalizes text-to-image models by incorporating the binary mask m as an explicit spatial control signal in conjunction with the text condition c , enabling the model to preserve contextual fidelity in unmasked regions while performing targeted generation within masked areas.

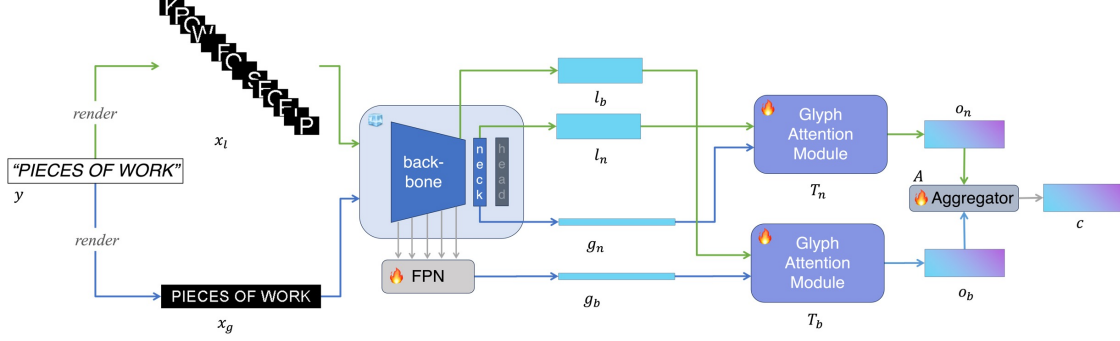


Figure 3. Complete model architecture of *GlyphMastero*. A specialized glyph encoder that introduces stroke-level precise control to the latent diffusion model for scene text editing.

3.2. Overall Architecture

We propose *GlyphMastero*, a novel glyph encoder that produces fine-grained glyph guidance for diffusion models in scene text editing. Relating to the general conditioning pipeline in Figure 2, our approach can be conceptualized as introducing a glyph encoder τ_θ to transform text conditions y into fine-grained glyph representations c to guide the denoising UNet to generate scene texts.

In contrast to prior works that directly utilize OCR features for diffusion model guidance - either as an augmentation [6, 24] to or a replacement [25] for natural language conditioning - without additional feature processing, our glyph encoder is a learnable and dedicated module that enhances feature representation through hierarchical processing. Our approach generates more fine-grained representations, significantly improving both text accuracy and style preservation in scene text generation.

Following [2], our work builds upon inpainting formulation as described in Eq.3 to operate at a region-specific granularity, as scene text editing naturally reduces to an inpainting problem where only the masked text regions require generation.

Our *GlyphMastero* is trained jointly with the latent diffusion model using the objective described in Eq.1, optimizing the glyph encoder directly through generation-based supervision.

3.3. Dual-Stream Glyph Integration

Figure 3 illustrates the overall architecture of our glyph encoder. Following [24], we incorporate the pretrained PaddleOCR-v4 [12] recognition model - which comprises a backbone, neck, and head - as our feature extractor for glyph images rendered from input texts. We extract two streams of glyph features with the OCR model: a local-level stream (depicted in green arrows) and a global-level stream (depicted in blue arrows), which we systematically integrate through cross-level and multi-scale fusion to derive fine-grained glyph guidance c .

In the local-level stream, given a text input y , we render a series of single-character glyph images, $x_l \in \mathbb{R}^{N \times H_l \times W_l}$, serving as the local-level representation of the text input. Here, N is the number of characters, and H_l and W_l are the height and width of each single character glyph image, respectively. The OCR model’s last-layer backbone output, l_b , and the neck output, l_n , form the local-level stream feature representations.

In the global-level stream, the input text y is rendered as a unified glyph image $x_g \in \mathbb{R}^{H_g \times W_g}$, where H_g and W_g denote the height and width dimensions, respectively. Similar to the local stream, the neck output feature, g_n , is extracted for subsequent processing. Unlike the local stream, we integrate M hierarchical backbone features ($M = 5$ in PaddleOCR-v4) for the global stream through a FPN [10], which fuses high-resolution, fine-grained features in shallow layers with semantic-rich features at lower resolutions in deeper layers, yielding the enhanced backbone features g_b .

Having extracted four features: l_n and l_b for the local-level stream, and g_n and g_b for the global-level stream, we then employ two glyph attention modules (Section 3.4) to capture interactions between local and global features for both the backbone and neck features. The cross-level interaction-enhanced features $o_n, o_b \in \mathbb{R}^{N \times d_o}$ are then obtained through two glyph attention modules T_n and T_b as follows:

$$o_n = T_n(l_n, g_n), \quad o_b = T_b(l_b, g_b) \quad (4)$$

where d_o represents the output dimension of glyph attention modules. We note that T_n and T_b share identical architectural designs; they are independently instantiated to process neck and backbone features respectively.

Finally, an aggregator A concatenates and projects the two features as follows:

$$c = A(o_b, o_n). \quad (5)$$

The resulting condition embedding $c \in \mathbb{R}^{N \times D}$, where

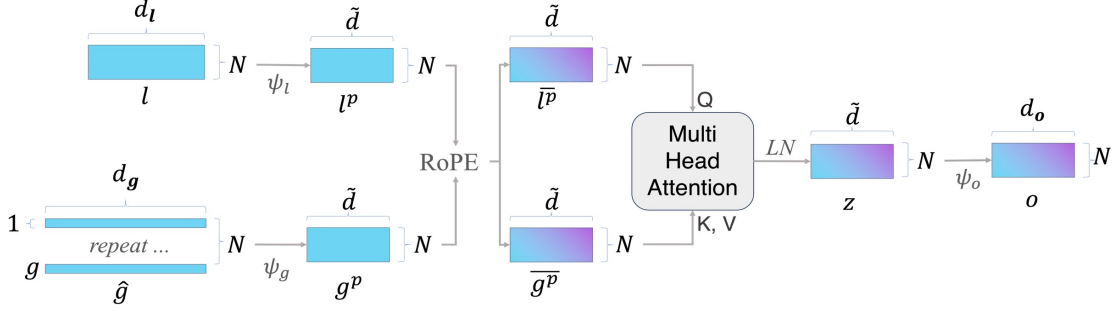


Figure 4. Glyph Attention Module

$D = d_o$, guides the UNet during both training and inference phases of scene text editing through cross-attention.

3.4. Glyph Attention Module

The intention of designing the glyph attention module is to use cross-attention to capture the interaction between character-level local features and line-level global features to get a better representation of text glyphs.

Figure 4 illustrates the details of our glyph attention module. Given the local features l and global features g extracted by the OCR model (where this notation applies to both backbone and neck levels, hence omitting the subscripts for notational simplicity). We first repeat the global feature $g \in \mathbb{R}^{1 \times d_g}$ by N times to obtain $\hat{g} \in \mathbb{R}^{N \times d_g}$ to match the local features $l \in \mathbb{R}^{N \times d_l}$ with respect to sequence length. Here N is the number of characters in the text input. The features l and \hat{g} are then projected to attention space dimension \tilde{d} through learnable linear transformations ψ_l and ψ_g , resulting in projected local and global features $l^p = \psi_l(l)$ and $g^p = \psi_g(\hat{g})$, both in $\mathbb{R}^{N \times \tilde{d}}$.

We add positional embeddings to the two streams of features with rotary positional embedding (RoPE) [22] by computing:

$$\bar{l}^p, \bar{g}^p = \text{RoPE}(l^p, g^p) \quad (6)$$

To capture interactions between local and global representations, we perform multi-head cross-attention where positionally encoded \bar{l}^p serves as queries and \bar{g}^p as keys and values, followed by a layer normalization (LN) to produce the attention map $z \in \mathbb{R}^{N \times \tilde{d}}$. Finally, a linear projection ψ_o is applied to map z from attention dimension \tilde{d} to the output size d_o with $o = \psi_o(z) \in \mathbb{R}^{N \times d_o}$.

4. Experiments

4.1. Dataset

For both training and experimental evaluation, we utilize AnyWord-3M [25], a comprehensive dataset designed for scene text generation and editing. We utilize the dataset specifically for scene text editing scenario: each sample is

an image containing multiple line-level annotations, which consists of text content, and its corresponding polygonal position as target area to generate new text. Since each image can have multiple text regions, we randomly sample one text-position pair in training. Our dataset formulation can be written as:

$$\mathcal{D} = \{(I_i, \{(T_{ij}, P_{ij})\}_{j=1}^{M_i})\}_{i=1}^N \quad (7)$$

where N is the total number of images, approximately 3.5 million in case of AnyWord dataset. M_i is number of text-position pairs in the i th image. Hence (T_{ij}, P_{ij}) is a single data sample, where T_{ij} represents the target text string and P_{ij} denotes its spatial location encoded as a quadrilateral polygon with four vertices. During training and evaluation, a binary mask is generated based on T_{ij} to delineate the text region for inpainting.

We evaluate our model using AnyText-Eval [25] for quantitative analysis (2000 images, 4181 English and 2092 Chinese text-position pairs) and a curated dataset of 80 challenging stylistic images (120 text-position pairs) for qualitative assessment. While AnyText-Eval provides statistical coverage, its target texts match the original, not fully reflecting real-world editing tasks. Our curated dataset focuses on challenging stylistic variations and incorporates new text contents.

4.2. Baseline Methods

For multi-lingual editing comparisons, we benchmark against state-of-the-art models DiffUTE [1] and AnyText [24]. For AnyText, we use the public AnyWord-3M checkpoint. We trained DiffUTE on AnyWord-3M for 15 epochs with a batch size of 256 and null condition probability of 0.1, matching our model’s hyperparameters.

Many existing methods primarily focused on English text, numbers, and punctuation editing. For English-only comparisons, we evaluated SRNet [26], MOSTEL [13], DiffSTE [6], TextDiffuser [2], and TextCtrl [29] using their publicly available checkpoints.

Prompt	Masked Source	DiffUTE	AnyText	Ours
Xiaxia				
Wen				
2024.12.07				
TEENAGER				
胸前 (in front of chest)				
赶海 (beachcombing)				
各位 (everybody)				

Figure 5. Qualitative comparison of scene text editing methods. Our GlyphMastero framework demonstrates superior text style preservation and content replacement accuracy. For Chinese cases (with English translations in brackets), our method achieves more precise text generation than DiffUTE and better style preservation than AnyText.

Model	Text Accuracy				Style Similarity			
	Sen.Acc \uparrow		CER \downarrow		FID \downarrow		LPIPS \downarrow	
	English	Chinese	English	Chinese	English	Chinese	English	Chinese
DiffUTE	0.3319	0.2523	0.3186	0.4048	14.3176	24.9295	0.1313	0.2056
AnyText	0.6067	0.5801	0.1730	0.2088	10.4257	24.9004	0.1098	0.1978
Ours	0.8170	0.7301	0.0741	0.1341	4.6101	11.8915	0.0545	0.1007

Table 1. Comparison with state-of-the-art multi-lingual (English and Chinese) methods. \uparrow/\downarrow indicates higher/lower is better. Our method outperforms previous works across all metrics.

4.3. Implementation Details

We initialize the UNet with Stable-Diffusion 2.1 inpainting weights [16]. And the pretrained OCR recognition model is initialized with PaddleOCR-v4 [12].

Each glyph attention module has one multi-head attention layer with 4 heads, with model size $\tilde{d} = 512$ and $d_o = 1024$. Their weights are initialized by Xavier initialization [20].

We implemented the FPN specifically suited for the PaddleOCR-V4’s backbone module. The module processes a hierarchical feature pyramid x_1, x_2, x_3, x_4, x_5 , where each feature map $x_i \in \mathbb{R}^{C_i \times H_i \times W_i}$ represents different levels of glyph features. Lateral connections first project all input features to a common hidden dimension D through 1×1 convolutions: $f_i : \mathbb{R}^{C_i \times H_i \times W_i} \rightarrow \mathbb{R}^{D \times H_i \times W_i}$. Starting from $p_5 = c_5$, for each level $i = 4, 3, 2, 1$, features are then fused as:

$$p_i = g_i(u(p_{i+1}) + c_i) \quad (8)$$

where $u(\cdot)$ denotes bilinear upsampling, g_i is a 3×3 convolution, and c_i represents lateral features. The final feature map undergoes channel projection, downsampling, and pooling to produce the enhanced global feature g_b with dimensions matching x_5 .

The guidance aggregator consists of two parallel linear projection branches that reduce the dimensionality of input embeddings from 1024 to 512 dimensions, then concatenating them back to 1024 dimensions.

Our model is trained for 15 epochs with a global batch size of 256 on 8 V100S-32G GPUs. We also use a null condition probability of 0.1 to allow classifier-free guidance (CFG) in inference. See the *Supplementary Material* for our analysis on effects of CFG in scene text editing task.

In inference, all methods use DDIM [21] sampler with 20 steps denoising steps, with CFG scale 9 for AnyText and 3 for ours and DiffUTE.

4.4. Quantitative Comparison

We measure four metrics for different methods: sentence accuracy (Sen.Acc) and character error rate (CER) for text content fidelity; Fréchet Inception Distance (FID) [19] and LPIPS [31] for style similarity. Sen.Acc measures line-level

Methods	Accuracy		Similarity	
	Sen.Acc \uparrow	CER \downarrow	FID \downarrow	LPIPS \downarrow
SRNet	0.3994	0.3802	27.00	0.1073
MOSTEL	0.5781	0.1984	50.24	0.4883
DiffSTE	0.5120	0.1993	14.06	0.1543
TextDiffuser	0.5260	0.2350	33.15	0.2406
DiffUTE	0.3319	0.3186	14.32	0.1313
AnyText	0.6067	0.1730	10.43	0.1098
TextCtrl	0.7654	0.0940	4.15	0.0425
Ours	0.8170	0.0741	4.61	0.0545

Table 2. English only quantitative comparison results.

accuracy, while CER is for character-level accuracy. FID measures distribution-level style similarity, while LPIPS focuses on sample-level similarity. We average LPIPS distances over all samples for the final measurement. FID and LPIPS are measured between cropped ground truth images and generated text regions.

Table 1 shows our comparisons with prior arts that has multi-lingual scene text editing capability. It is seen that our method significantly outperforms prior arts in both text generation accuracy and style similarity. Our overall sentence accuracy (averaging English and Chinese results) is 48.14% and 18.02% higher than DiffUTE and AnyText, respectively; CER is 25.76% and 8.68% lower. For style similarity, we also achieved with substantially lower FID and LPIPS distances compared to DiffUTE and AnyText. For FID evaluations, our method’s distance is 57.95% lower than DiffUTE, and 53.28% lower than AnyText, on average. Our LPIPS distance is 53.93% lower than DiffUTE, and 49.54% lower than AnyText.

Table 2 presents English-only comparison results. Our method achieved the highest accuracy metrics while outperforming all other methods in similarity measures except TextCtrl, which showed marginally better FID and LPIPS. We also evaluated our approach on TextCtrl’s ScenePair dataset (1,285 test cases), using their GitHub-published results and evaluation scripts, also achieving favorable outcomes. Full comparison results are available in the *Supplementary Material*.

4.5. Qualitative Comparison

Figure 5 presents comparative results among our method, AnyText, and DiffUTE. Our approach demonstrates sub-

Component	Text Accuracy				Style Similarity			
	Sen.Acc \uparrow		CER \downarrow		FID \downarrow		LPIPS \downarrow	
	English	Chinese	English	Chinese	English	Chinese	English	Chinese
Full model	0.5494	0.5120	0.1766	0.2367	30.9095	51.3762	0.1190	0.2134
– FPN	0.4536	0.3698	0.2470	0.3314	32.4550	53.0127	0.1247	0.2208
– T_b	0.5065	0.4271	0.2128	0.2987	30.5866	49.6588	0.1196	0.2110
– T_n w/ l_n	0.3263	0.2735	0.3137	0.3916	30.6271	51.6288	0.1211	0.2121
w/ g_n	0.1003	0.0719	0.5727	0.6579	34.7661	51.5788	0.1412	0.2334

Table 3. Ablation study results. When removing T_n , we experiment with two scenarios: using local features (l_n) and global features (g_n).

stantial improvements over prior arts in both text accuracy and style preservation. We specifically include Chinese characters in our evaluation as they present a more rigorous test case, featuring complex glyph structures with multiple strokes. The superior performance in accurately generating these intricate characters demonstrates our GlyphMastero’s effectiveness in capturing stroke-level precision features. More extensive qualitative results are available in the *Supplementary Material*.

4.6. Ablation Studies

To evaluate the effectiveness of individual components, we conducted a systematic ablation study on GlyphMastero. The experiments are performed using a subset of 375K images from the Anyword-3M dataset, with training conducted for 15 epochs using a batch size of 256 on four NVIDIA A100-40GB GPUs. Ablation study results are recorded in Table 3.

First, we removed the FPN that fuses multi-scale backbone feature maps, and replaced it with the final backbone layer output in global-level stream. The model trained with this modification led to a 22.42% drop in average sentence accuracy for English and Chinese texts and a 28.54% increase in CER (Table 3). These results demonstrate that fusing high-resolution features from shallow layers with semantic-rich features from deeper layers significantly impacts the generated text quality.

Next, we removed the backbone glyph attention module T_b , retaining only the neck glyph attention module T_n for cross-level feature capture. This resulted in a 13.68% drop in average sentence accuracy and a 19.20% increase in CER (Table 3) compare to the full model. Notably, removing both FPN and T_b yielded better performance than removing FPN alone. We attribute this to the FPN’s role in adaptively refining features for T_b ’s cross-level feature capture. Without FPN, T_b struggles to effectively process directly extracted backbone features.

Finally, we removed T_n and used only neck features as guidance, testing two scenarios. First, with position-embedded local neck features l_n (w/ l_n), we observed a 43.49% drop in average sentence accuracy and 41.40%

increase in CER. These significant degradations highlight the crucial role of our glyph attention module in capturing local-global feature relationships. Second, using global neck features g_n as prior guidance (w/ g_n) - equivalent to AnyText’s OCR feature utilization - yielded the poorest results. We attribute this to g_n prior reducing embedding length from N to 1, while local neck features l_n maintained length N .

The style similarity metrics (FID and LPIPS) remain consistent throughout ablation experiments, with only slight variations. This stability aligns with GlyphMastero’s core function as a glyph encoder, where its components focus on providing fine-grained glyph guidance, while style preservation is primarily handled by the latent diffusion inpainting model’s inherent capacity for maintaining local visual consistency.

5. Conclusion & Limitations

We present *GlyphMastero*, a novel trainable glyph encoder that advances scene text editing through effective modeling of hierarchical relationships between local character-level features and global text-line structures. Our approach addresses the challenge of encoding complex glyph structures through multi-scale feature incorporation and explicit modeling of hierarchical glyph relationships. The effectiveness of our approach is demonstrated by an 18.02% improvement in sentence accuracy compare to the previous state-of-the-art method and significant enhancement in style preservation, with text-region FID reduced by 53.28%.

One limitation of our approach is that accuracy for generating long text, though improved over prior work, still lags behind shorter text. We attribute this to training data limited to 512×512 resolution and constraints of the base latent diffusion model. Future work will explore higher-resolution training and more robust base models to address this limitation.

6. Acknowledgement

Xiaolin Hu was supported by the National Natural Science Foundation of China (No. U2341228).

References

- [1] Haoxing Chen, Zhuoer Xu, Zhangxuan Gu, Jun Lan, Xing Zheng, Yaohui Li, Changhua Meng, Huijia Zhu, and Weiqiang Wang. Diffute: Universal text editing diffusion model. In *Advances in Neural Information Processing Systems 36: Annual Conference on Neural Information Processing Systems 2023, NeurIPS 2023, New Orleans, LA, USA, December 10 - 16, 2023*, 2023. 2, 5
- [2] Jingye Chen, Yupan Huang, Tengchao Lv, Lei Cui, Qifeng Chen, and Furu Wei. Textdiffuser: Diffusion models as text painters. In *Advances in Neural Information Processing Systems 36: Annual Conference on Neural Information Processing Systems 2023, NeurIPS 2023, New Orleans, LA, USA, December 10 - 16, 2023*, 2023. 2, 3, 4, 5
- [3] Ian J. Goodfellow, Jean Pouget-Abadie, Mehdi Mirza, Bing Xu, David Warde-Farley, Sherjil Ozair, Aaron C. Courville, and Yoshua Bengio. Generative adversarial nets. In *Advances in Neural Information Processing Systems 27: Annual Conference on Neural Information Processing Systems 2014, December 8-13 2014, Montreal, Quebec, Canada*, pages 2672–2680, 2014. 2
- [4] Jonathan Ho, Ajay Jain, and Pieter Abbeel. Denoising diffusion probabilistic models. In *Advances in Neural Information Processing Systems 33: Annual Conference on Neural Information Processing Systems 2020, NeurIPS 2020, December 6-12, 2020, virtual*, 2020. 2, 3
- [5] Qirui Huang, Bin Fu, Aozhong Zhang, and Yu Qiao. Gen-text: Unsupervised artistic text generation via decoupled font and texture manipulation. *CoRR*, abs/2207.09649, 2022. 2
- [6] Jiabao Ji, Guanhua Zhang, Zhaowen Wang, Bairu Hou, Zhifei Zhang, Brian Price, and Shiyu Chang. Improving diffusion models for scene text editing with dual encoders. *CoRR*, abs/2304.05568, 2023. 2, 4, 5
- [7] Diederik P. Kingma and Max Welling. Auto-encoding variational bayes. In *2nd International Conference on Learning Representations, ICLR 2014, Banff, AB, Canada, April 14-16, 2014, Conference Track Proceedings*, 2014. 3
- [8] Junyeop Lee, Yoonsik Kim, Seonghyeon Kim, Moonbin Yim, Seung Shin, Gayoung Lee, and Sungrae Park. Rewritenet: Realistic scene text image generation via editing text in real-world image. *CoRR*, abs/2107.11041, 2021. 2
- [9] Minghao Li, Tengchao Lv, Jingye Chen, Lei Cui, Yijuan Lu, Dinei A. F. Florêncio, Cha Zhang, Zhoujun Li, and Furu Wei. Trocr: Transformer-based optical character recognition with pre-trained models. In *Thirty-Seventh AAAI Conference on Artificial Intelligence, AAAI 2023, Thirty-Fifth Conference on Innovative Applications of Artificial Intelligence, IAAI 2023, Thirteenth Symposium on Educational Advances in Artificial Intelligence, EAAI 2023, Washington, DC, USA, February 7-14, 2023*, pages 13094–13102. AAAI Press, 2023. 2, 3
- [10] Tsung-Yi Lin, Piotr Dollár, Ross B. Girshick, Kaiming He, Bharath Hariharan, and Serge J. Belongie. Feature pyramid networks for object detection. In *2017 IEEE Conference on Computer Vision and Pattern Recognition, CVPR 2017, Honolulu, HI, USA, July 21-26, 2017*, pages 936–944. IEEE Computer Society, 2017. 2, 4
- [11] Jian Ma, Mingjun Zhao, Chen Chen, Ruichen Wang, Di Niu, Haonan Lu, and Xiaodong Lin. Glyphdraw: Learning to draw chinese characters in image synthesis models coherently. *CoRR*, abs/2303.17870, 2023. 3
- [12] PaddlePaddle. PP-OCRv4. https://github.com/PaddlePaddle/PaddleOCR/blob/release/2.7/doc/doc_ch/PP-OCRv4_introduction.md, 2023. Accessed: 2024-07-31. 4, 7
- [13] Yadong Qu, Qingfeng Tan, Hongtao Xie, Jianjun Xu, YuXin Wang, and Yongdong Zhang. Exploring stroke-level modifications for scene text editing. In *Thirty-Seventh AAAI Conference on Artificial Intelligence, AAAI 2023, Thirty-Fifth Conference on Innovative Applications of Artificial Intelligence, IAAI 2023, Thirteenth Symposium on Educational Advances in Artificial Intelligence, EAAI 2023, Washington, DC, USA, February 7-14, 2023*, pages 2119–2127. AAAI Press, 2023. 2, 5
- [14] Alec Radford, Jong Wook Kim, Chris Hallacy, Aditya Ramesh, Gabriel Goh, Sandhini Agarwal, Girish Sastry, Amanda Askell, Pamela Mishkin, Jack Clark, Gretchen Krueger, and Ilya Sutskever. Learning transferable visual models from natural language supervision. In *Proceedings of the 38th International Conference on Machine Learning, ICML 2021, 18-24 July 2021, Virtual Event*, pages 8748–8763. PMLR, 2021. 2
- [15] Colin Raffel, Noam Shazeer, Adam Roberts, Katherine Lee, Sharan Narang, Michael Matena, Yanqi Zhou, Wei Li, and Peter J. Liu. Exploring the limits of transfer learning with a unified text-to-text transformer. *J. Mach. Learn. Res.*, 21: 140:1–140:67, 2020. 3
- [16] Robin Rombach, Andreas Blattmann, Dominik Lorenz, Patrick Esser, and Björn Ommer. High-resolution image synthesis with latent diffusion models. In *IEEE/CVF Conference on Computer Vision and Pattern Recognition, CVPR 2022, New Orleans, LA, USA, June 18-24, 2022*, pages 10674–10685. IEEE, 2022. 3, 7
- [17] Olaf Ronneberger, Philipp Fischer, and Thomas Brox. U-net: Convolutional networks for biomedical image segmentation. In *Medical Image Computing and Computer-Assisted Intervention - MICCAI 2015 - 18th International Conference Munich, Germany, October 5 - 9, 2015, Proceedings, Part III*, pages 234–241. Springer, 2015. 3
- [18] Prasun Roy, Saumik Bhattacharya, Subhankar Ghosh, and Umapada Pal. STEFANN: scene text editor using font adaptive neural network. In *2020 IEEE/CVF Conference on Computer Vision and Pattern Recognition, CVPR 2020, Seattle, WA, USA, June 13-19, 2020*, pages 13225–13234. Computer Vision Foundation / IEEE, 2020. 2
- [19] Maximilian Seitzer. pytorch-fid: FID Score for PyTorch. <https://github.com/mseitzer/pytorch-fid>, 2020. Version 0.3.0. 7
- [20] Justin A. Sirignano and Konstantinos Spiliopoulos. Scaling limit of neural networks with the xavier initialization and convergence to a global minimum. *CoRR*, abs/1907.04108, 2019. 7

- [21] Jiaming Song, Chenlin Meng, and Stefano Ermon. Denoising diffusion implicit models. In *9th International Conference on Learning Representations, ICLR 2021, Virtual Event, Austria, May 3-7, 2021*. OpenReview.net, 2021. [7](#)
- [22] Jianlin Su, Yu Lu, Shengfeng Pan, Bo Wen, and Yunfeng Liu. Roformer: Enhanced transformer with rotary position embedding. *CoRR*, abs/2104.09864, 2021. [5](#)
- [23] Roman Suvorov, Elizaveta Logacheva, Anton Mashikhin, Anastasia Remizova, Arsenii Ashukha, Aleksei Silvestrov, Naejin Kong, Harshith Goka, Kiwoong Park, and Victor Lempitsky. Resolution-robust large mask inpainting with fourier convolutions. In *IEEE/CVF Winter Conference on Applications of Computer Vision, WACV2022, Waikoloa, HI, USA, January 3-8, 2022*, pages 3172–3182. IEEE, 2022. [3](#)
- [24] Yuxiang Tuo, Wangmeng Xiang, Jun-Yan He, Yifeng Geng, and Xuansong Xie. Anytext: Multilingual visual text generation and editing. *CoRR*, abs/2311.03054, 2023. [2](#), [3](#), [4](#), [5](#)
- [25] Yuxiang Tuo, Wangmeng Xiang, Jun-Yan He, Yifeng Geng, and Xuansong Xie. Anytext: Multilingual visual text generation and editing. In *The Twelfth International Conference on Learning Representations, ICLR 2024, Vienna, Austria, May 7-11, 2024*. OpenReview.net, 2024. [2](#), [4](#), [5](#)
- [26] Liang Wu, Chengquan Zhang, Jiaming Liu, Junyu Han, Jing-tuo Liu, Errui Ding, and Xiang Bai. Editing text in the wild. In *Proceedings of the 27th ACM International Conference on Multimedia, MM 2019, Nice, France, October 21-25, 2019*, pages 1500–1508. ACM, 2019. [2](#), [5](#)
- [27] Qiangpeng Yang, Jun Huang, and Wei Lin. Swaptxt: Image based texts transfer in scenes. In *2020 IEEE/CVF Conference on Computer Vision and Pattern Recognition, CVPR 2020, Seattle, WA, USA, June 13-19, 2020*, pages 14688–14697. Computer Vision Foundation / IEEE, 2020. [2](#)
- [28] Yukang Yang, Dongnan Gui, Yuhui Yuan, Weicong Liang, Haisong Ding, Han Hu, and Kai Chen. Glyphcontrol: Glyph conditional control for visual text generation. In *Advances in Neural Information Processing Systems 36: Annual Conference on Neural Information Processing Systems 2023, NeurIPS 2023, New Orleans, LA, USA, December 10 - 16, 2023*, 2023. [3](#)
- [29] Weichao Zeng, Yan Shu, Zhenhang Li, Dongbao Yang, and Yu Zhou. Textctrl: Diffusion-based scene text editing with prior guidance control. In *Advances in Neural Information Processing Systems 38: Annual Conference on Neural Information Processing Systems 2024, NeurIPS 2024, Vancouver, BC, Canada, December 10 - 15, 2024*, 2024. [5](#)
- [30] Lvmin Zhang, Anyi Rao, and Maneesh Agrawala. Adding conditional control to text-to-image diffusion models. In *IEEE/CVF International Conference on Computer Vision, ICCV 2023, Paris, France, October 1-6, 2023*, pages 3813–3824. IEEE, 2023. [2](#)
- [31] Richard Zhang, Phillip Isola, Alexei A Efros, Eli Shechtman, and Oliver Wang. The unreasonable effectiveness of deep features as a perceptual metric. In *CVPR*, 2018. [7](#)

GlyphMastero: A Glyph Encoder for High-Fidelity Scene Text Editing

Supplementary Material

7. Effects of Classifier-Free Guidance

Classifier-free guidance (CFG) has demonstrated effectiveness in controlling the strength of prompt-following behavior in text-to-image diffusion models. Recognizing its potential utility in scene text editing, we incorporate CFG by training our model with a probabilistic null glyph condition (we also trained DiffUTE with CFG for fair comparison, though not in their original work).

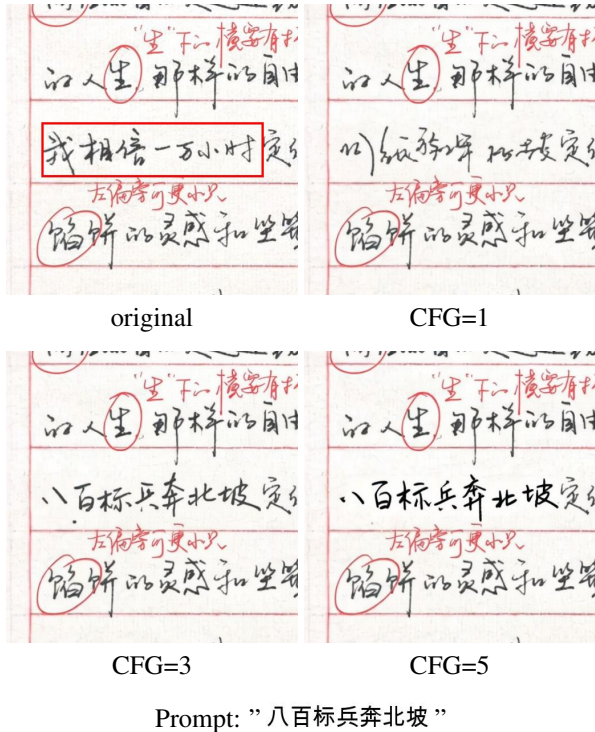


Figure 6. Effect of classifier-free guidance (CFG). Original image with target area mask shown top-left. Without CFG (i.e. CFG=1), GlyphMastero produces unreadable text. CFG=3 improves readability while maintaining style. CFG=5 generates overly thick text, deviating from the original region.

Our experiments with CFG reveal a crucial trade-off in scene text editing. As demonstrated in Figure 6, we found that in inference, a higher CFG scale results in stronger glyph control, producing clearer and thicker text. This allows for improved readability when editing texts. However, our findings show that this comes at a cost to style preservation. Conversely, lower CFG scales excel at maintaining the original text style, though occasionally at the expense of target text accuracy. This insight offers a new approach to balancing readability and style preservation in the scene

text editing task.

8. Example Failure Cases

As shown in Figure 7, our method encounters limitations when the selected editing region substantially exceeds the target text length. In such scenarios, the model struggles to maintain coherent text generation, resulting in irregularly sized characters and occasional repetition patterns in the output. These artifacts emerge as the model attempts to distribute textual elements across disproportionately large spatial regions.



Figure 7. Example of a failure case. The upper image displays the source text with regions marked by red boxes. The middle and bottom images show two unsuccessful generation attempts. The intended target text appears at the bottom left of each generated result.

9. Additional Results

9.1. Quantitative Comparison

To cross-validate the effectiveness of our method, we also evaluated our method on TextCtrl’s ScenePair dataset (1,285 test cases), re-evaluating all other methods using TextCtrl’s GitHub-published results and scripts. Table 4 showed our superior generation accuracy and strong performance across style metrics, except for a slightly higher FID.

9.2. Qualitative Comparison

We present additional qualitative comparisons in Figure 8, 9, 10, and 11.

Figure 8 presents additional examples from our curated test set, demonstrating the efficacy of our approach for stylistic scene text editing. Additionally, Figures 9 and 10

Methods	Accuracy		Similarity			
	W.Acc \uparrow	NED \uparrow	SSIM \uparrow	PSNR \uparrow	MSE \downarrow	FID \downarrow
SRNet	16.64	0.4790	26.66	14.08	5.61	49.23
MOSTEL	35.16	0.5570	27.46	14.46	5.19	49.20
DiffSTE	29.14	0.5255	26.91	13.49	6.07	118.60
TextDiffuser	51.48	0.7190	27.02	13.99	5.72	57.48
AnyText	47.97	0.7186	31.19	13.58	6.36	52.07
TextCtrl	78.91	0.9199	37.93	14.92	4.58	31.98
Ours	83.52	0.9572	47.58	16.25	3.97	32.03

Table 4. Performance comparison on English *ScenePair* testset. SSIM and MSE scaled by $\times 10^{-2}$. W.Acc: Word Accuracy.

showcase random samples from the AnyText-Eval benchmark dataset - Figure 9 illustrates our model’s performance on English text using the LAION dataset, while Figure 10 highlights its capabilities with Chinese text from the Wukong dataset. Figure 11 provides comparative results on TextCtrl’s ScenePair test set as previously discussed. These qualitative results align consistently with our quantitative evaluations, validating the effectiveness of our proposed method.





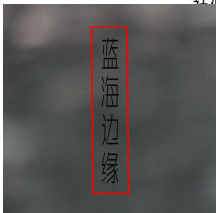

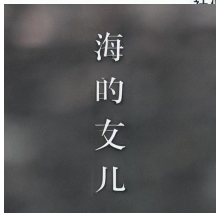
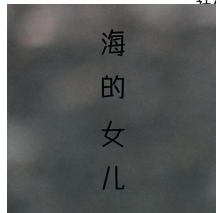












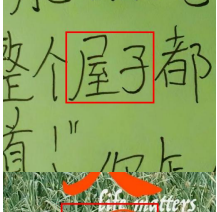
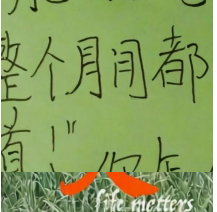
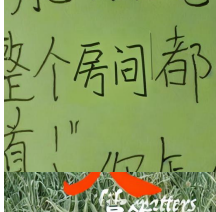
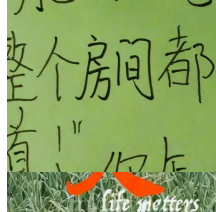




Prompt	Masked Source Image	DiffUTE	AnyText	Ours
2026-03-09				
海的女儿 (the daughter of the sea)				
34				
羊 (sheep)				
喜多多 (Xi'duo'duo)				
房间 (room)				
世间 (the world)				

Figure 8. Comparison results on our test set with stylish scene texts

Prompt	Masked Source Image	DiffUTE	AnyText	Ours
WINNER				
DANCE				
200				
IC				
HITS				
S				
Strategic				

Figure 9. Comparison results on English (LAION) test set

Prompt	Masked Source Image	DiffUTE	AnyText	Ours
注意安全 (watch out)				
小仙女专用座 (dedicated seat for girls)				
帮人难处： (help others)	<p>帮人难处：</p> <p>锦上添花易，雪中送炭难！ 我们应该在别人 困难之时帮扶一把， 不管别人是否记得， 自己要做到无愧于心。</p>	<p>帮人难处：</p> <p>锦上添花易，雪中送炭难！ 我们应该在别人 困难之时帮扶一把， 不管别人是否记得， 自己要做到无愧于心。</p>	<p>帮人难处：</p> <p>锦上添花易，雪中送炭难！ 我们应该在别人 困难之时帮扶一把， 不管别人是否记得， 自己要做到无愧于心。</p>	<p>帮人难处：</p> <p>锦上添花易，雪中送炭难！ 我们应该在别人 困难之时帮扶一把， 不管别人是否记得， 自己要做到无愧于心。</p>
居住证 (residency ID)				
先进集体 (advanced group of people)				
精度高圆板牙 (high precision bolt)				
寓 (apartment)				

Figure 10. Comparison results on Chinese (Wukong) test set

Source Image	Target Text	SRNet	MOSTEL	DiffSTE	TextDiffuser	AnyText	TextCtrl	GlyphMaster
	"Learning"							
	"Buses"							
	"FLASH"							
	"ROYAL"							
	"Bernd"							
	"and"							
	"WEATHER"							
	"EU-funded"							
	"SPRINKLER"							
	"FOSTERS"							
	"HAMBLION"							
	"Centre"							
	"DRIVERS"							
	"WSDL"							
	"Authorised"							
	"National"							
	"Section"							
	"Centre"							
	"order"							
	"LONG"							
	"work"							
	"PLEASE"							
	"Knowledge"							
	"and"							
	"EMMERICH"							

Figure 11. Comparison of different scene text editing methods on the ScenePair dataset